Catal Lett (2008) 120:288–293
DOI 10.1007/s10562-007-9282-7

Effect of Crystal Size on Physico-Chemical Properties of ZSM-5

Madhulika Singh · Raviraj Kamble · Nagabhatla Viswanadham

Received: 14 August 2007 / Accepted: 12 September 2007 / Published online: 2 October 2007

Abstract In an attempt to produce a ZSM-5 type material with ample mesoporosity as well as micro porosity and improved external surface area, the nanocrystalline ZSM-5 (NZ) was synthesized. The material NZ was characterized by a variety of physical techniques and its properties were compared with that of micrometer range ZSM-5 (HZ). Improvement in pore volume along with mesoporosity is observed in NZ. Though there is an improvement in micropore volume, the mesopores with diameter > 100 Å have mainly contributed to the improved pore volume in NZ. The organic template used in NZ synthesis decomposed at two different temperatures in DTA/TGA studies suggesting the additional role of template in mesopore formation in NZ. The NZ exhibited relatively lower acidity, but has greater amount of strong acidity when compared to HZ.

Keywords Nano ZSM-5 · Mesoporous ZSM-5 · DTA/TG · Organic template

1 Introduction

The zeolite ZSM-5, of structural type MFI (Mobil Five) is a medium pore size zeolite. This molecular sieve is synthesized from hydro gels containing precursors of Si and Al at high temperature and autogenous pressure [1]. ZSM-5 exemplifies a continuing area of research and interest in the processes involving petrochemicals and petroleum refining [2–4]. However it is a micro porous material with a pore diameter 5.5 Å and this limits its ability to catalyze bigger molecules having critical size greater than this diameter. For this a pore channel of mesopore range is required so that the reactant molecule can come in contact with the acid sites. Research is on to come up with newer techniques for the generation of mesoporous ZSM-5 material. The notable options in this regard include dealumination of micro porous material through combined effect of steaming and acid leaching or desilication by treatment in alkaline medium to create 'opened' channels. These post synthesis treatments dissolve amorphous material and can generate spectacular mesoporosity but a non-uniform and/or severe dealumination/desilication may lead to crystal collapse [5–7]. In one method the mesoporosity is obtained by occlusion of small (12–18 nm nano-sized) carbon particles into the crystal during the synthesis and subsequently removing them through oxidation [8–10]. The almost striking option for obtaining mesoporosity could be the systematic decrease of the crystal size from micro domain range to nano scale domain size so as to obtain intercrystalline mesoporosity. The transition from micro to nano crystallinity can be envisioned as the transition of extended symmetry of atoms of the crystal to just few unit cells. Thus there is an increased ratio of atoms at or near the surface relative to the number of atoms on the inner part of the crystal. The added advantage of this method is that the smaller crystal of zeolite has larger surface areas and less diffusion limitations compared with the zeolite of micrometer range [11].

In the present paper we have studied the contrast in the physicochemical characteristics of the micro and the nano sized ZSM-5. A special attention is given to understand the porosity changes in the ZSM-5 when it goes from micro to nano particle range.

M. Singh · R. Kamble · N. Viswanadham (✉)
Catalysis and Conversion Process Division,
Indian Institute of Petroleum, Dehradun 248005, India
e-mail: nvish@iip.res.in; nviswanadham@india.com

2 Experimental

2.1 Zeolite Preparation

In both the synthesis described below we aimed to produce ZSM-5 in which the framework Al is in the fixed amount equivalent to an atomic Si/Al ratio of 30. In the synthesis of micrometer ZSM-5 (HZ) we followed the procedure given in patented literature [1] and for nano-sized ZSM-5 (NZ) the procedure given by Van Grieken et al. [12] was followed. In both the syntheses tetra ethyl ortho silicate (TEOS) was used as silica source, aluminium nitrate (s.d. fine chem. Ltd.) as an alumina source and tetra propyl ammonium hydroxide (TPAOH, 20 wt.% in water, Merck) as a structure directing agent.

2.1.1 Synthesis of HZ

In this synthesis sodium silicate (Merck) was used as silica source. Sodium hydroxide was added slowly to sodium silicate solution and after that Al source and then template TPAOH was added drop wise. The components were mixed with constant stirring at room temperature. The pH of the resulting gel was then adjusted to 10.5 by adding 1:1 H_2SO_4 solution before charging it in Teflon lined autoclave for hydrothermal synthesis at 180 °C for 3 days. The product thus formed was filtered and washed with deionised water.

2.1.2 Synthesis of NZ

In this synthesis Tetra ethyl ortho silicate (TEOS, Merck) was used as silica source. TEOS being an organic silica source is supposed to come in the aqueous phase slowly. Al source was added slowly to precooled TPAOH solution and after that TEOS was added drop wise. The components were mixed with constant stirring. After adding all the ingredients the solution was left to hydrolyze at room temperature for 41 h. The gel thus obtained was heated at 80 °C to evaporate water and ethanol formed during the hydrolysis of TEOS and to obtain a concentrated gel. The concentrated gel was charged in a Teflon lined autoclave for hydrothermal synthesis as in case of HZ. The synthesis was performed at 170 °C for duration of 2 days.

The output of this synthesis was a colloidal suspension of the zeolite on the mother liquor. This showed the Tyndall light scattering effect and a very slow sedimentation rate. Typically no sedimentation was observed by keeping the solution as such for 2 days. Recovery of solids from this highly stable suspension was obtained by centrifuging at a very high speeds and times after diluting with water (water:suspension ratio 4 by weight) to lower the viscosity and pH.

Both as synthesized samples were calcined at 500 °C for 4 h. under vacuum.

3 Characterization Methods

X-ray powder diffraction (XRD) pattern were measured on Rigaku Dmax III B equipped with rotating anode and CuKα radiations. The measurements were conducted in continuous $\theta/2\theta$ scan refraction mode. The anode was operated at 30 KV and 15 mA the 2θ angles were measured 5°–60° at the rate of 2°/min.

The N_2 adsorption desorption isotherms were measured at 77 K on ACAP Micrometrics USA instrument. Before measurement the samples were evacuated overnight at 250 °C. The BET surface area was calculated from linear part of plot according to IUPAC recommendations [13]. The reported external surface area and micro pore surface area and volume of the zeolite samples NZ and HZ were estimated from slopes and intercepts respectively of t-plots derived from N_2 adsorption isotherms. The Thermal Gravimetric Analysis (TG) and the Differential Thermal Analysis (DTA) figures of as synthesized uncalcined samples were recorded on Pyris Diamond TG/DTA Analyzer in the temperature range 50–1,000 °C with heating rate of 10 °C/min in N_2 gas atmosphere. The Scanning Electron Microscope (SEM) pictures were recorded on Hitachi-S250 instrument. Acidity was characterized on heat flow microcalorimeter model Setaram C-80, attached to a volumetric adsorption unit for probe delivery. About 0.1 g of catalyst was outgassed at 723 K under vacuum. The microcalorimetric measurement for ammonia adsorption was carried out at 448 K. Differential heat of ammonia adsorption was determined by introducing small quantity of ammonia on to the outgassed sample, till the neutralization of all acid sites occurred on the catalyst surface. The resulting thermograms for each dose of ammonia gave the heat of adsorption and pressure change gave the amount of ammonia adsorbed [14].

4 Results and Discussion

The XRD spectra is a finger print of the zeolite structure but here the XRD peaks of the two ZSM-5 samples NZ and HZ shown in Fig. 1 are characteristically different. While in NZ the peaks are broader and largely attenuated and in HZ they are sharp. However both XRD patterns depicted exhibits a very low background signal and sharp reflections indicating excellent crystallanity of both the samples. The decrease in peak intensity and increase in line width in case of NZ can be attributed to decrease in crystal size [15].

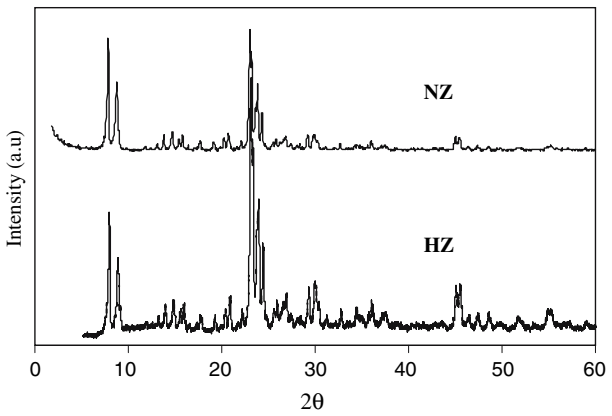

Fig. 1 XRD patterns of zeolites

The TG/DTG/DTA studies also indicated the differences in NZ and HZ samples (Fig. 2a, b). While there are three sharp peaks in the temperature ranges 100–150 °C, 200–300 °C and 400–500 °C in case of nano ZSM-5 (Fig. 2a) there are only two peaks in temperature ranges 100–150 °C and 400–500 °C in case of normal ZSM-5 (Fig. 2b). The first endothermic peak in the region 100–150 °C can be assigned to desorption of occluded water in both the zeolites. The third exothermic peak which is also common in both cases is assigned to TPA^+ cations balancing $Al(OSi)_4^-$ [16]. The second peak which is an exothermic, is observed only incase of NZ, but not by HZ. This peak can be assigned to the TPA^+ cations balancing

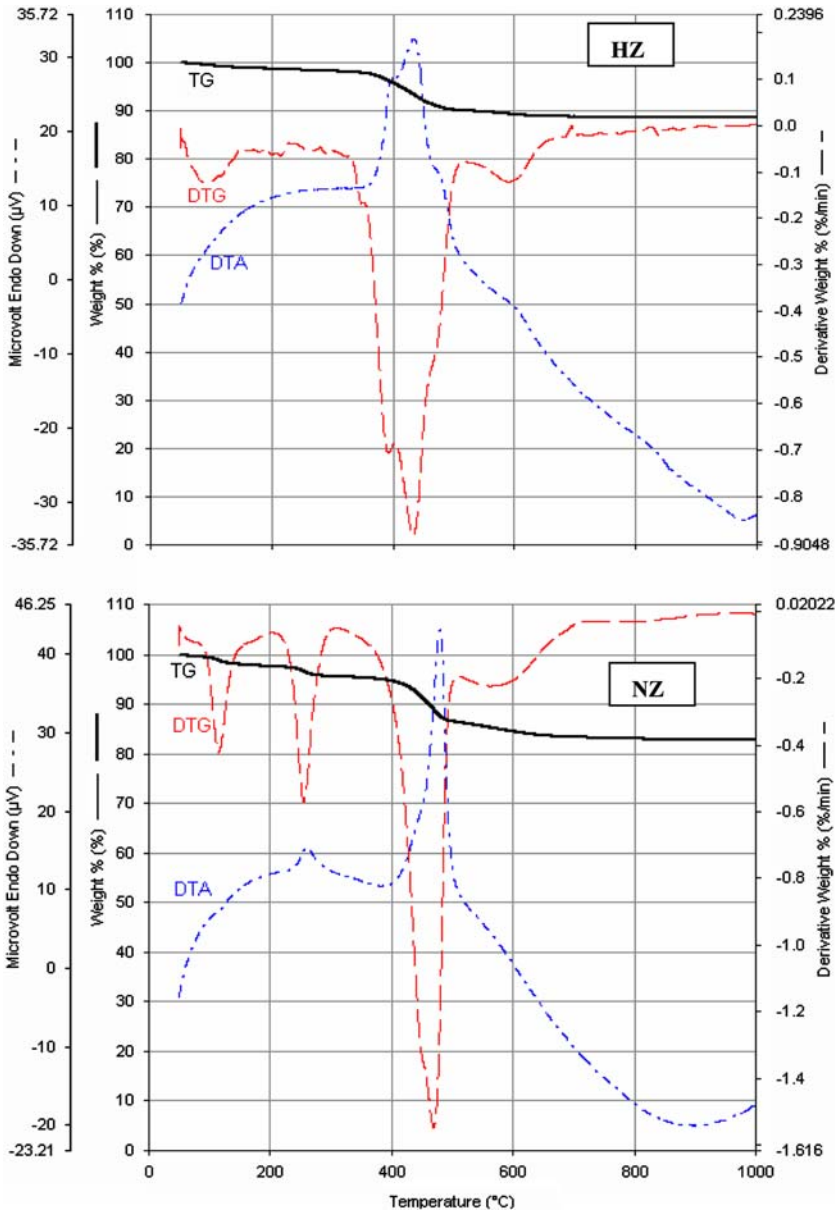

Fig. 2 TG/DTG/DTA of zeolites

the charge of Si–O^- groups in the connectivity defects and not due to occluded TPAOH. This is because TPAOH is strongly basic which gets completely ionized in water during hydrothermal synthesis. This peak appears only in case of nano ZSM-5 may be postulated due to the presence of excess amine used in the synthesis of nano ZSM-5. Thus the role of excess amine in the synthesis of nanocrystalline ZSM-5 can be envisioned as being two fold, the structurally specific "pore directing" role and structurally non specific "pore filling" role leading to the formation of inter crystalline voids.

The decrease in crystal size is also evident from the very large increase in external surface area. This is based on the common principle that as the size of the crystal for same quantity (x g) of the sample decreases, the total external surface area increases. An excellent correlation between external surface area and crystal size has been given by Song et al. [17].

However the model accounts the correlation between silicalite and purely siliceous form of ZSM-5. The same model can be applicable to the zeolite synthesized in the present study. Since the Al–O–Al bond length is slightly longer (1.75 Å) than that of Si–O–Si bond length (1.62 Å) the error incurred in assuming atoms whose all silica material can be neglected when Si/Al ratio is 30. In this model the shape of the crystal is assumed to be cubic having size x nm and external surface area $6x^2$ nm^2. Silicalite-1 has MFI framework structure with unit cell volume of 5.21 nm^3 and chemical formula 96 Si:192 O, giving weight 5,856. Thus for Sillicalite-1 crystals with x nm size the chemical formula weight can be calculated as

$$(x^3/5.21)5856 = 1127x^3$$

For 1 g silicallite the total external surface area is then

$$6x^2 \times 6.02 \times 10^{23}/\ 1127x^3$$

Thus after consideration of unit conversions the external surface area of silicalite crystal is

$$S_{ext.} = 3214/x$$

where, $S_{ext.}$ is external surface area in m^2/g and x is silicalite-1 crystal size in nm.

Thus following the above calculations, the size of the crystal of our NZ sample comes out to be ~150 nm which corroborates with the result concluded from SEM analysis of the sample Fig. 3. The size of microcrystalline ZSM-5 is ~5,000 nm.

The nano ZSM-5 sample shows mesoporosity and this is evident in the adsorption/desorption isotherm as shown in Fig. 3. There is a steep jump in the isotherm and a big desorption loop in case of NZ while this particular feature is absent from the isotherm of HZ samples. The

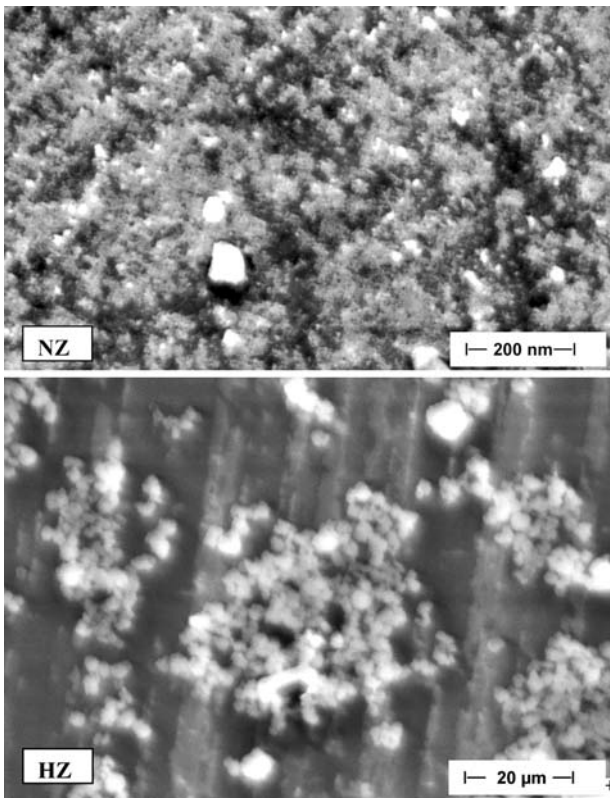

Fig. 3 Scanning electron micrographs of zeolites

hysteresis loop of NZ appears at a high relative pressure (P/P_0 = 0.9–1.0) and reflects intercrystalline voids in the packing of the smaller crystals [17]. Thus in normal ZSM-5 most of the surface and volume corresponds to zeolitic micropore but in nano a large share of surface can be assigned to the external ones, namely the super micropore as well as mesopore.

This is also evident from Figs. 4 and 5, which show increased micro porosity in NZ and also that there is a

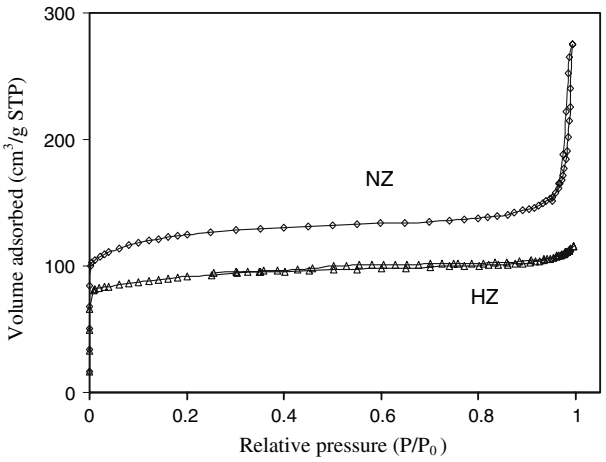

Fig. 4 Adsorption/desorption isotherms of zeolites

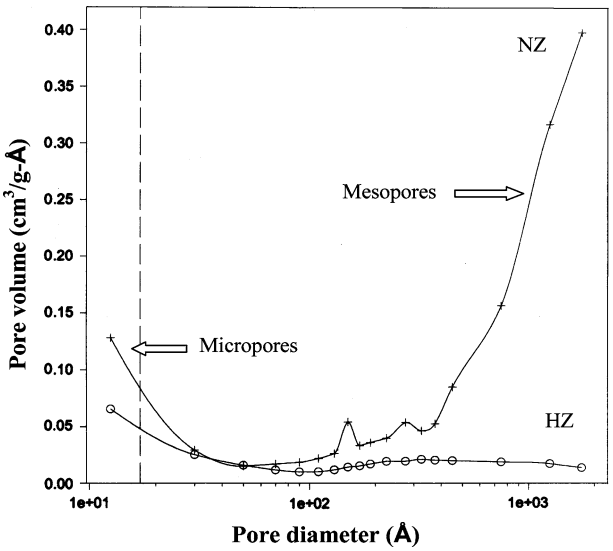

Fig. 5 BJH Pore size distribution curves of zeolites

pecking order of porosity which can only be due to inter-crystalline space. This also means heterogeneity in crystal size and their aggregation though all crystals are in nano range. Thus, microporous system of ZSM-5 promotes to the one having a range of pore sizes as we tend towards nanocrystalline size. In such a material one can expect the loss of shape selectivity, leading to the off-putting consequences on desired product distribution. However, it is known that the presence of acid sites outside the zeolite channels is negligible so the non-shape selective reactions catalyzed on the surface acid sites may be insignificant. Table 1 compares the acidity pattern of NZ and HZ. The acidity has been categorized in three classes, namely strong, medium and weak based on the heat of adsorption of ammonia. The acid sites showing the heat of adsorption value greater than 100 kJ/mol is a strong acid site while the one having the value between 100 kJ/mol and 75 kJ/mol is a medium and the ones having even less than this value are weak acid sites. Thus it is evident from the table that total acid sites of NZ are less but the amount of strong acid sites is more. Moreover, in NZ the intra-crystalline diffusion barriers are supposed to be much less because of lower size of the crystal and hence it may be expected to show better activity for most of the typical reactions catalyzed by ZSM-5 such as light paraffin aromatization. This multiporous material can also prove to be of great interest in sorptive separation processes [18–21].

5 Summary

The physicochemical properties of ZSM-5 depend on the crystal size and these clearly differentiate nanocrystalline material from microcrystalline material where the number of crystals per crystallite decreases. The nanocrystalline particles do not affect strongly the crystallinity of the zeolite as measured by XRD. DTA thermogram of nano ZSM-5 is illustrating the presence of template in two different environments that suggesting the additional role of template in the formation mesopores. The nano material has also shown a fascinating increase in pore volume and external surface area. Thus a decrease in crystal size to the nano range can convert an inherently micro porous system of ZSM-5 to the one showing a hierarchy of pore sizes. Thus, under these conditions a shift towards nano

Table 1 Physicochemical properties of zeolites

Surface area and pore volume						
Samples	BET surface area (m^2/g)	Micro pore (<20 Å) area (m^2/g)	External surface area (m^2/g)	Total pore volume (cm^3/g)	Micro pore volume (cm^3/g)	
HZ	345.7	255.8	89.9	0.1763	0.1022	
NZ	461.1	322.9	138.2	0.3855	0.1321	
Volume (cm^3/g) in pores of various diameter (Å)						
	<10 Å	10–20 Å	20–100 Å	100–200 Å	200–500 Å	>500 Å
HZ	0.1262	0.0134	0.0143	0.0039	0.0079	0.0105
NZ	0.1637	0.0269	0.0176	0.0097	0.0220	0.1464
Micro calorimetric acidity (m mol NH_3/g zeolite)						
	Total	Strong (ΔH > 100 kJ/mol)	Medium (ΔH = 100–75 kJ/mol)	Weak (ΔH < 75 kJ/mol)		
NZ	0.42	0.16	0.13	0.13		
HZ	0.79	0.05	0.42	0.32		

crystallinity from micro crystallinity the material obtained shows a larger concentration of sites with strong Bronsted acidity and both large inter particle mesoporosity and a relatively large micro porosity.

Acknowledgements Authors are thankful to Director, IIP for his support and encouragement during this research work. One of the authors, R.K. acknowledges CSIR for awarding the Junior Research Fellowship.

References

1. Argauer RJ, Landolt GR (1972) US Patent 3702886 Mobil Co
2. van der Pol AJHP, Verduyn AJ, van Hooff JHC (1992) Appl Catal A: Gen 92:113
3. Viswanadham N, Shido T, Sasaki T, Iwasawa Y (2002) J Phys Chem 106:10955
4. Viswanadham N, Gupta JK, Muralidhar G, Garg MO (2006) Energy Fuels 1806
5. Triantafillidis CS, Vlessidis AG, Nalbendian L, Evmiridis NP (2001) Micropor Mesopor Mater 47:369
6. Groen JC, Jansen JC, Moulijin JA, Parez-Ramirez J (2004) Colloid Surf A 241:13062
7. Suzuki T, Okuhara T (2001) Micropor Mesopor Mater 43:83
8. Jansen AH, Schmidt I, Jacobsen CJH, Koster AJ, de Jong KP (2003) Micropor Mesopor Mater 65:59
9. Chou YH, Cundy CS, Garforth AA, Zholobenko VL (2005) Micropor Mesopor Mater 89:78
10. Jacobsen CJH, Madsen C, Houzvicka J, Schmidt I, Carlsson A (2000) J Am Chem Soc 122:7116
11. Schmidt T (2000) Inorg Chem 39:2279
12. Van Grieken R, Sotelo JL, Menendez JM, Melero JA (2000) Micropor Mesopor Mater 39:155
13. Sing KSW, Everett DH, Haul RAW, Moscon L, Picrotti RA, Ranquerol J, Sieminiewiska T (1985) Pure Appl Chem 57:603
14. Viswanadham N, Dixit L, Gupta JK, Garg MO (2006) J Mol Catal 258:15
15. Song W, Justice RE, Jones CA, Grassian VH, Larsen SC (2004) Langmuir 20:4696
16. Camblor MA, Corma A, Valencia S (1998) Micropor Mesopor Mater 25:59
17. Chou YH, Cundy CS, Garforth AA, Zholobenko VL (2006) Micropor Mesopor Mater 89:78
18. Stout SC, Larsen SC, Grassian VH (2007) Micropor Mesopor Mater 100:77
19. Whang Y, Tang Y, Dong A, Wang X, Ren N, Shan W, Gao Z (2002) Adv Mate 14:994
20. Sun J, Shen Z, Maschmeyer T, Moulijin JA, Coppens MO (2001) Chem Commun 2676
21. Davis ME (2002) Nature 417:813